

# Atomic scale friction between clean graphite surfaces

Katuyoshi Matsushita

*Department of Physics, Graduate School of Science, Osaka University,  
1-1 Machikaneyama, Toyonaka, Osaka, 560-0043, Japan\**

Hiroshi Matsukawa

*Department of Physics, College of Science and Engineering, Aoyama Gakuin University,  
5-10-1 Huchinobe, Sagamihara, Kanagawa, 229-8558, Japan†*

Naruo Sasaki

*Department of Applied Physics, Faculty of Engineering, Seikei University,  
3-3-1 Kichijoji-kitamachi, Musashino-shi, Tokyo 180-8633, Japan and  
Precursory Research for Embryonic Science and Technology (PRESTO),  
Japan Science and Technology Corporation (JST)  
4-1-8 Honcho, Kawaguchi-shi, Saitama 332-0012, Japan‡*

## Abstract

We investigate atomic scale friction between clean graphite surfaces by using molecular dynamics simulation. The simulation reproduces atomic scale stick-slip motion and low frictional coefficient, both of which are observed in experiments using frictional force microscope. We clarify the microscopic mechanism of the low frictional coefficient of graphite.

PACS numbers: 07.79.Sp; 46.30.Pa; 31.15.Qg

Keywords: Atomic scale friction, Graphite, Molecular dynamics simulation, Frictional force microscope

---

\*Electronic address: kmatsu@presto.phys.sci.osaka-u.ac.jp

†Electronic address: hm@phys.aoyama.ac.jp

‡Electronic address: naru@cello.mm.t.u-tokyo.ac.jp

Investigation of atomic scale friction is important for the understanding of fundamental mechanisms of macroscopic friction and for many fields of engineering such as nanomachine[1]. Frictional force microscope (FFM) has played an important role in study of atomic scale friction[1, 2]. Behavior of frictional force in FFM experiments has been studied theoretically and numerically based on the model which consists of a single atom tip and potential of a substrate surface[3, 4, 5, 6, 7, 8, 9, 10]. On the other hand some groups pointed out that a flake cleaved from the substrate plays an important role in frictional phenomena of FFM experiments in layered materials[2, 6, 11, 12]. It is not appropriate to discuss frictional phenomena with a flake by using the single atom tip model. We investigate atomic scale friction between clean graphite surfaces by molecular dynamics simulation. The model employed here describes friction in FFM experiments on a graphite substrate with a flake. The present work enables us to understand frictional phenomena in FFM experiment more deeply. Graphite is one of the most important solid lubricants. We also clarify the microscopic origin of friction and lubrication properties of graphite.

The model consists of a monolayer graphite substrate, a monolayer graphite flake and a spring which drives the flake as shown in fig. 1(a). Atoms in the substrate are fixed and those in the flake obey the following eq. of motion,

$$m_C \ddot{x}_i^\alpha = -\gamma \dot{x}_i^\alpha - \frac{\partial V_{\text{Sub}}}{\partial x_i^\alpha} - \frac{\partial V_I}{\partial x_i^\alpha} - \frac{k_\alpha}{N_f} (x_C^\alpha - x_B^\alpha). \quad (1)$$

Here  $m_C$  is the mass of the carbon atom,  $x_i^\alpha$ ,  $\alpha = x, y, z$ , are components of the  $i$ -th atom position vector and a dot above  $x_i^\alpha$  denotes the time derivative. The  $x$  and  $y$ -directions are shown in fig. 1(b) and the  $z$ -direction is normal to the surface plane of the substrate. The first term in the r. h. s. of eq. (1) is a damping term proportional to the velocity, which reproduces the energy dissipation to an external environment such as degrees of the freedom of atoms in the substrate. We set a damping constant  $\gamma = 1.14 \times 10^{-4}$  nNs/m. This value of  $\gamma$  holds the stability of the flake for the time step of MD simulation  $\Delta t = 2.74 \times 10^{-15}$  sec. The second term denotes the force coming from interatomic interactions between the flake and the substrate.  $V_{\text{Sub}}$  denotes the sum of pair atomic interaction potential between an atom in the flake and that in the substrate. We employ the Lennard-Jones (12, 6) potential,

$$V_{\text{Sub}} = \sum_{r_{i,j} < R} \varepsilon \left[ \left( \frac{\sigma}{r_{i,j}} \right)^{12} - \left( \frac{\sigma}{r_{i,j}} \right)^6 \right]. \quad (2)$$

Here  $r_{i,j}$  is a distance between the  $i$ -th atom in the flake and the  $j$ -th atom in the substrate. The index of the summation “ $r_{i,j} < R$ ” indicates that the pair of the summation is restricted to that with

their distance  $r_{i,j}$  being less than a cut off length  $R$ . We set  $\varepsilon = 0.965 \times 10^{-2}$  eV,  $\sigma = 0.340$  nm and  $R = 2.0$  nm. The above values of  $\varepsilon$  and  $\sigma$  are often employed in the interlayer atomic potential in bulk graphite [13]. The third term denotes the force by the intraflake atomic interactions and  $V_I$  is assumed as,

$$V_I = \frac{\mu_r}{2} \sum_{\langle i,j \rangle} (r_{i,j} - a)^2 + \frac{\mu_\theta}{2} \sum_{\langle i:j,k \rangle} a^2 (\theta_{i:j,k} - \theta_0)^2 + \frac{\mu_p}{2} \sum_{\langle i:j,k,l \rangle} \left( \delta z_i - \frac{\delta z_j + \delta z_k + \delta z_l}{3} \right)^2. \quad (3)$$

Here the indices of the summation  $\langle i, j \rangle$ ,  $\langle i : j, k \rangle$  and  $\langle i : j, k, l \rangle$  denote a nearest-neighbor bond, a pair of nearest-neighbor bond around the  $i$ -th atom and a set of all nearest-neighbor bonds around the  $i$ -th atom, respectively. The variables,  $r_{i,j}$ ,  $\theta_{i:j,k}$  and  $\delta z_i$ , denote the length of the nearest neighbor bond, the angle between the bonds  $\langle i, j \rangle$  and  $\langle i, k \rangle$  and the normal displacement of the  $i$ -th atom, respectively. The parameters of  $V_I$  are set as  $\mu_r = 4.1881 \times 10^3$  eV/nm<sup>2</sup>,  $a = 0.14210$  nm,  $\mu_\theta = 0.29959 \times 10^3$  eV/nm<sup>2</sup>,  $\theta_0 = 2\pi/3$  and  $\mu_p = 1.8225 \times 10^3$  eV/nm<sup>2</sup>, respectively. This potential was employed in the study of lattice vibrations and specific heat of graphite [14] and FFM images [7, 8]. The fourth term denotes the force by the driving spring with the components of a spring constant,  $k_\alpha$ ,  $\alpha = x, y, z$ . The spring corresponds to a tip and a cantilever in FFM.  $x_C^\alpha$ ,  $x_B^\alpha$  and  $N_f$  denote a component of a center position of the flake mass, a component of a base position of the driving spring and the number of carbon atoms in the flake, respectively. Here we set  $k_x = k_y = 1.5$  eV/nm<sup>2</sup>,  $k_z = 5.0$  eV/nm<sup>2</sup> and  $N_f = 110$ . The shape of the flake is shown in fig. 1(b).  $\vec{x}_B$  obeys the following eq. of motion,

$$R_C m_C \ddot{x}_B^z = -\gamma \dot{x}_B^z - L + k_z (x_C^z - x_B^z). \\ \dot{x}_B^x = V_S^x, \quad \dot{x}_B^y = V_S^y, \quad (4)$$

Here  $R_C$ , the ratio of the effective mass of the tip and the cantilever to the mass of the carbon atom, is assumed to be 100.0.  $L$  and  $(V_S^x, V_S^y)$  denote a loading force and a lateral driving velocity, respectively. The values of these parameters are kept constant during driving.

Equations of motion, (1) and (4) are solved numerically by using the Runge-Kutta method. The initial state is a stable state of  $\vec{x}_B$  and the flake on the substrate with a loading force  $L$  without lateral expansions of the driving spring. The configuration corresponds to a AB stacking structure of bulk graphite as shown in fig.1(b). A frictional force is defined as a driving direction component of the force of the driving spring,  $k_\alpha (x_B^\alpha - x_C^\alpha)$ .

In our calculation two features of the driven flake are observed. First, deformations of the flake are negligibly small. This is because that the interlayer atomic interactions between the flake and the substrate under load in our calculation are much weaker than the intralayer atomic interactions in the flake. Second, rotation of the flake around the position of the center of the flake mass  $\vec{x}_C$  in the  $x$ - $y$  plane is inhibited due to the substrate potential barriers against it.

Due to the above two features the dynamics of the center of the flake mass,  $\vec{x}_C$ , governs the dynamics of the system. Here we focus on the typical motions of  $\vec{x}_C$ . Figure 2 shows the driving direction component of the center of the flake mass,  $x_C$ , as a function of the driving direction component of the base position of the driving spring,  $x_B$ , for  $L = 100$  nN,  $|\vec{V}_S| = 0.22$  m/s in the case driven along the  $x$  (a) and  $y$  (b) directions, respectively. The stick-slip motion of  $\vec{x}_C$  is observed. The periods of the stick-slip motion in the case driven along the  $x$  and  $y$ -directions agree with the periods of the graphite lattice in each direction, 0.426 and 0.246 nm, respectively.

Figure 3 shows trajectories of  $\vec{x}_C$  in the  $x$ - $y$  plane for  $L = 100$  nN,  $|\vec{V}_S| = 0.22$  m/s. The contour lines denote equipotential lines of the substrate potential. The motion of  $\vec{x}_C$  starts from the initial position A. The solid line in the figure denotes the trajectory of  $\vec{x}_C$  in the case driven along the  $x$ -direction. At first  $\vec{x}_C$  goes slowly to the position B. As soon as  $\vec{x}_C$  arrives at B,  $\vec{x}_C$  slips to the next sticking position close to D through the position C, both of which are the positions of the substrate potential minimum. The sticking time around D is much shorter than that around A due to large elongation of the driving spring along the  $y$ -direction. As soon as  $\vec{x}_C$  arrives at E,  $\vec{x}_C$  slips again close to I, which is equivalent to A. Then  $\vec{x}_C$  repeats the periodic stick-slip motion. The dashed line shown in the figure denotes the trajectory of  $\vec{x}_C$  in the case driven along the  $y$ -direction. At first  $\vec{x}_C$  goes slowly to the position F. As soon as  $\vec{x}_C$  arrives at F,  $\vec{x}_C$  slips to the next sticking position close to G, which is the position of the substrate potential minimum. The sticking time around G is shorter than that around A due to elongation of the driving spring along the  $x$ -direction. As soon as  $\vec{x}_C$  arrives at H, the flake slips again to the next sticking position close to J, which is equivalent to A. Then  $\vec{x}_C$  repeats the periodic stick-slip motion and the trajectory of  $\vec{x}_C$  becomes zigzag. Thus the stick-slip motions of  $\vec{x}_C$  occur between positions close to the substrate potential minimum, in which the flake makes the stacking structure of the graphite, and at the stick positions with largest sticking time the flake makes the AB stacking structure of bulk graphite with the substrate as shown in the inset of fig. 3. The atomic scale stick-slip motion results from the binding of the flake close to the stacking positions of the graphite flake on the graphite substrate.

Figure 4 shows the frictional force  $F$  as a function of  $x_B$  for  $|\vec{V}_S| = 0.22$  m/s in the case driven along the  $x$  (a) and  $y$  (b) directions, respectively.  $F$  initially increases linearly with  $x_B$  due to the elastic deformation of the driving spring. After  $F$  takes the maximum value the curves exhibit the periodic saw-tooth shape due to the periodic stick-slip motions of the flake. The periods of the saw-tooth behavior in the case driven along the  $x$  and  $y$ -directions agree with those, 0.426 and 0.246 nm, in the stick-slip motion of  $\vec{x}_C$ , respectively.

We define the maximum static frictional force  $F_s$  and the kinetic frictional force  $F_k$  as the maximum frictional force during driving and a time averaged value of the frictional force during one cycle of the stick-slip motion, respectively. Figure 5 shows  $F_s$  and  $F_k$  as a function of the loading force,  $L$ , in the case driven along the  $x$  and  $y$ -directions. The values of the frictional forces in fig. 5 are obtained by extrapolating data for  $|\vec{V}_S| = 0.22, 0.44$  and  $0.88$  m/s to  $|\vec{V}_S| = 0$  m/s for the comparison with experiments, in which the typical magnitude of  $\vec{V}_S$  is about 40 nm/s. The dependence of  $F_s$  and  $F_k$  on  $|\vec{V}_S|$  is weak.  $F_s$  and  $F_k$  linearly depend on the loading force and have a finite adhesive term  $a$ , which is the frictional force at  $L = 0$  nN. The frictional coefficient  $\mu$  is defined as,

$$\tilde{F} = \mu L + a. \quad (5)$$

Here  $\tilde{F}$  denotes  $F_s$  or  $F_k$ . The magnitude of the frictional force in the range of the loading force in fig. 5 is very low with the frictional coefficients  $\mu_s = \mu_k = 0.013$  and  $\mu_s = \mu_k = 0.0055$  in the case driven along the  $x$  and  $y$ -directions, respectively. Here  $\mu_s$  and  $\mu_k$  denote the frictional coefficients of  $F_s$  and  $F_k$ , respectively. The values are close to those observed in the experiment,  $\mu = 0.012$  [2].

Here we discuss the origin of the low frictional coefficient of graphite. It is believed that the low frictional coefficient of macroscopic graphite surfaces or graphite solid lubricants results from the weak interlayer interaction. We obtain, however, the frictional coefficient  $\mu = 0.099$  in the case of a single carbon atom tip on the graphite substrate, which is much larger than those in our simulation of the flake and that in the experiment[2]. The difference of the frictional coefficients indicates an another mechanism of the low frictional coefficient between graphite surfaces.

In the flake there are two kinds of lattice sites  $\hat{A}$  and  $\hat{B}$  catching different forces from the substrate as shown in fig. 6. The substrate potential for the flake  $V_{\text{sub}}$  is equal to the sum of the substrate potential for a single atom at the sites  $\hat{A}$ ,  $V_{\text{sub}}^{\hat{A}}$ , and that at the sites  $\hat{B}$ ,  $V_{\text{sub}}^{\hat{B}}$ . That is,

$$V_{\text{sub}} = N_{\hat{A}} V_{\text{sub}}^{\hat{A}} + N_{\hat{B}} V_{\text{sub}}^{\hat{B}}, \quad (6)$$

where  $N_{\hat{A}}$  and  $N_{\hat{B}}$  denote the number of the sites  $\hat{A}$  and  $\hat{B}$ . In the flake  $N_{\hat{A}} = N_{\hat{B}}$ . Here we consider the case that  $\vec{x}_C$  moves straight between the nearest substrate potential minimums A and C shown in fig. 3. The atoms at sites  $\hat{A}$  move from the potential minimum to the maximum and those at sites  $\hat{B}$  move from the maximum to the minimum as shown in fig. 7. During the motion the increase of  $V_{\text{sub}}^{\hat{A}}$  and the decrease of  $V_{\text{sub}}^{\hat{B}}$  cancel out each other. Then the substrate potential for the flake  $V_{\text{sub}}$  does not vary in the route between the nearest potential minimums. As a result the flat potential valleys appear for the flake in the shaded region shown in fig. 3. The valleys enable the flake to move easily and yield low frictional force. Due to this mechanism graphite becomes a good lubricant with low frictional coefficient. On the other hand the single carbon atom above the graphite substrate has large frictional coefficient because of the absence of such cancellation mechanism of the substrate potential.

In the present work we have investigated atomic scale friction between clean graphite surfaces by the numerical simulation. The simulation reproduces atomic scale stick-slip motion and low frictional coefficients. The former is due to the binding of the flake close to the stacking configurations on the substrate. The latter results from the cancellation of the forces coming from the substrate between two kinds of lattice sites in the flake.

We express sincere thanks to Profs. K. Miura and S. Morita for valuable discussions. The present work is financially supported by Grant-in-Aid for Scientific Research from Japan Society for the Promotion of Science.

- 
- [1] B. N. J. Persson, *Sliding Friction: Physical Principles and Applications*, Springer, Berlin, (1998).
  - [2] C. M. Mate, G. M. McClelland, R. Erlandsson and S. Chiang, *Phys. Rev. Lett.*, **59**, 1942, (1987).
  - [3] S. Fujisawa, E. Kishi, Y. Sugawara and S. Morita, *Nanotechnology*, **4**, 138, (1993).
  - [4] S. Fujisawa, Y. Sugawara and S. Morita, *Jpn. J. Appl. Phys.*, **35**, 5909, (1996).
  - [5] S. Fujisawa, E. Kishi, Y. Sugawara and S. Morita, *Phys. Rev. B*, **58**, 4909, (1998).
  - [6] S. Morita, S. Fujisawa and Y. Sugawara, *Surf. Sci. Rep.*, **23**, 1, (1995).
  - [7] N. Sasaki, K. Kobayashi and M. Tsukada, *Phys. Rev. B*, **54**, 2138, (1996).
  - [8] N. Sasaki, M. Tsukada, S. Fujisawa, Y. Sugawara, S. Morita and K. Kobayashi, *J. Vac. Sci. Technol. B*, **15**, 1479, (1997).
  - [9] N. Sasaki, M. Tsukada, Y. Sugawara, S. Morita and K. Kobayashi, *Phys. Rev. B*, **57**, 3785, (1998).

- [10] H. Hölscher, U. D. Schwarz, O. Zwörner, and R. Wiesendanger, *Phys. Rev. B*, **57**, 2477, (1998).
- [11] K. Miura and S. Kamiya, *Europhys. Lett.*, **58** 610, (2002).
- [12] K. Miura, S. Kamiya and N. Sasaki, *Phys. Rev. Lett.*, **90**, 055509, (2003).
- [13] See i. e. H. Rafii-Taber, *Phys. Rep.*, **325**, 239, (2000).
- [14] A. Yoshimori and Y. Kitano, *J. Phys. Soc. Jap.*, **11**, 352, (1956)

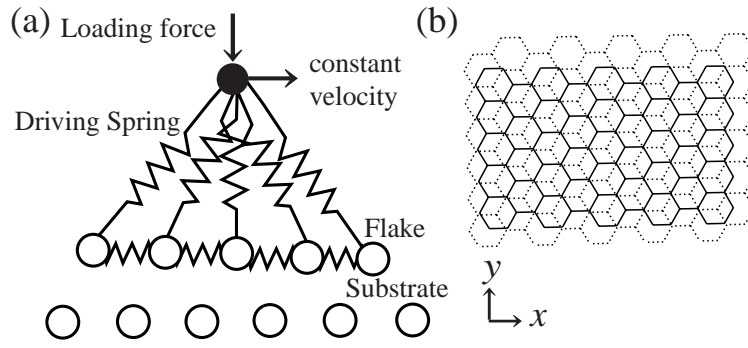


FIG. 1: (a)The schematic illustration of the model and (b) the flake and the substrate in the present study. The solid and dashed lines in (b) denote bonds in the flake and those in the substrate, respectively.

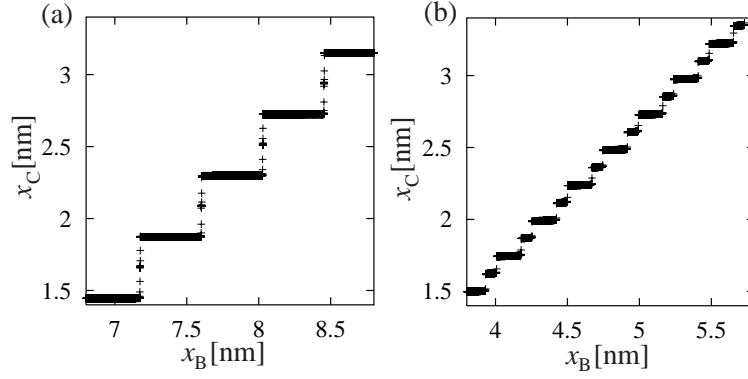


FIG. 2:  $x_C$  as a function of  $x_B$  in the case driven along the (a)  $x$  and (b)  $y$ -directions for  $L = 100$  nN,  $|\vec{V}_S| = 0.22$  m/s. The data are plotted by the constant time interval  $\delta t = 300 \Delta t$ , where  $\Delta t$  denotes the time step of the simulation.



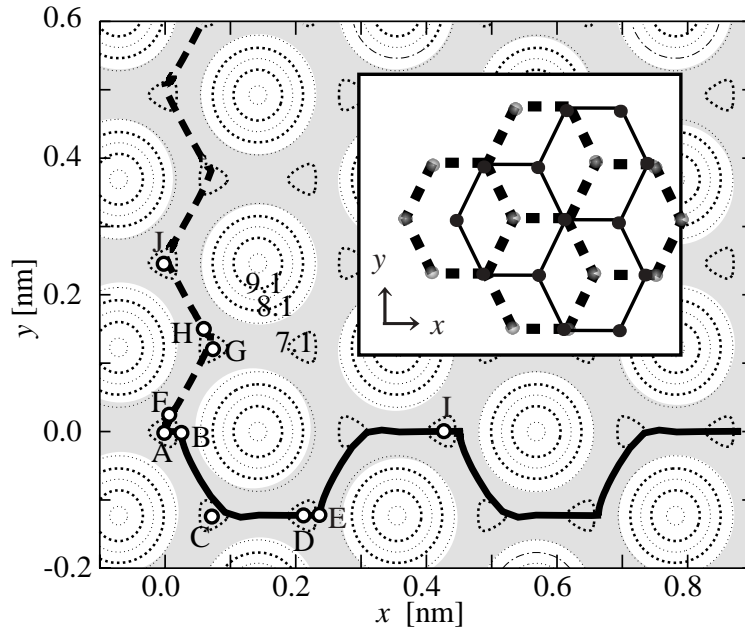


FIG. 3: The trajectories of  $\vec{x}_C$  for  $L = 100$  nN,  $|\vec{V}_S| = 0.22$  m/s. The solid and dashed lines indicate the trajectories of  $\vec{x}_C$  in the case driven along the  $x$  and  $y$ -directions, respectively. The heavy and thin dotted lines indicate the equipotential lines of the substrate potential as a function of  $\vec{x}_C$  in the  $x$ - $y$  plane under the condition that the separation between the flake and the substrate is set to the constant value, 0.273 nm, which is equal to the time averaged value of the separation during driving for  $L = 100$  nN. The unit of numbers on heavy dotted equipotential lines is eV. The inset shows the configuration of the flake and the substrate which makes the AB stacking structure of bulk graphite. The solid and dashed lines in the inset denote the bonds in the flake and the substrate, respectively. The shaded region denotes potential valleys.

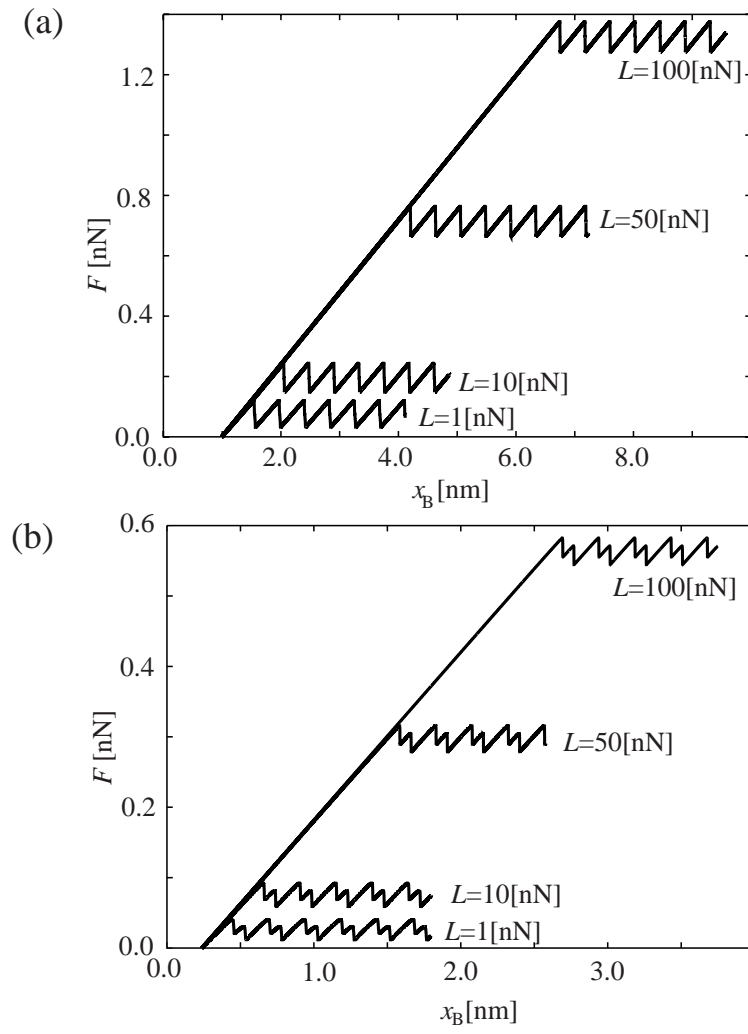


FIG. 4: A frictional force  $F$  as a function of  $x_B$  for  $|\vec{V}_S| = 0.22$  m/s and  $L = 1, 10, 50$  and  $100$  nN and in the case driven along the (a)  $x$  and (b)  $y$ -directions.

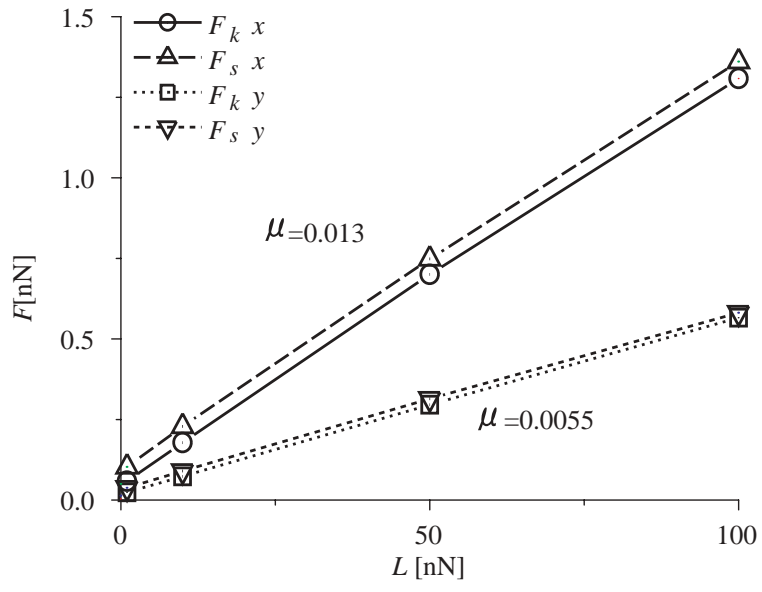


FIG. 5:  $F_k$  and  $F_s$ , as a function of the loading force.  $x$  and  $y$  indicate the direction of the driving.

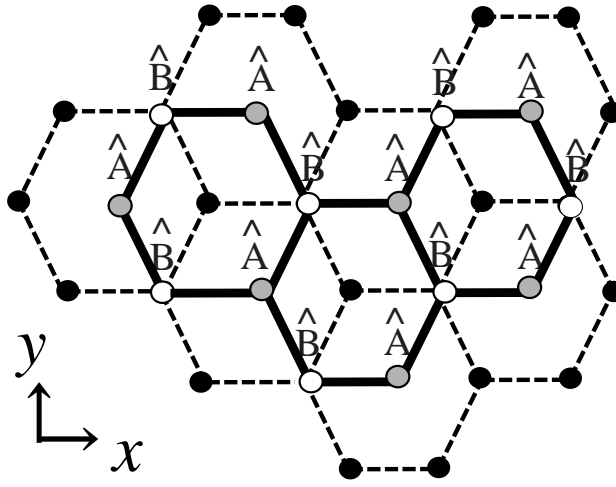


FIG. 6: The stacking structure of a flake on a substrate. The solid and dashed lines denote bonds in the flake and those in the substrate. The sites of carbon atoms  $\hat{A}$  and  $\hat{B}$  catch different forces of the interatomic interactions between the flake and the substrate.

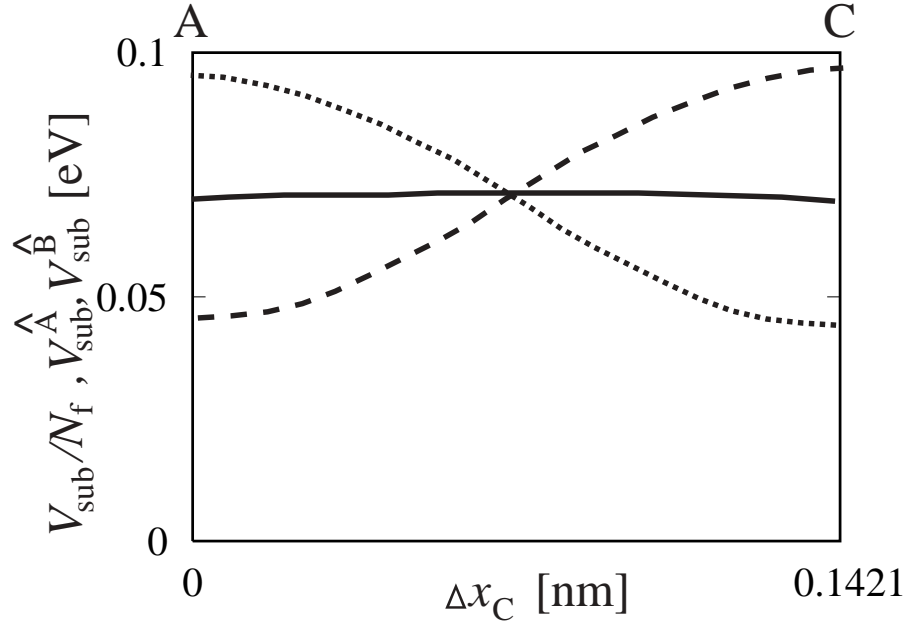


FIG. 7: The substrate potential during the motion of the flake  $A \rightarrow C$  shown in fig. 3. The solid, dashed and dotted lines denote the potential value per atom for the flake as a function of a moving-direction displacement of  $\vec{x}_C$ ,  $\Delta x_C$ , and the potential value as a function of  $\Delta x_C$  for a single atom at the sites  $\hat{A}$  and  $\hat{B}$ , respectively.